546925

POPULAR SUMMARY

Precipitation Anomalies in the Tropical Indian Ocean and Possible Links to the Initiation of El Niño

by

Scott Curtis JCET/UMBC
Robert Adler NASA/GSFC
George Huffman SSAI

Everyone is familiar with the climate phenomenon "El Niño" and the havoc it causes to weather around the globe. Scientists, using sophisticated computer models and observations of temperature, winds, and clouds are trying to forecast when an El Niño will occur. Sometimes, if the conditions are right, enhanced precipitation and winds move from the eastern Indian Ocean to the central Pacific and may trigger an El Niño event. Models have difficulty predicting El Niño in part because they have difficulty predicting these propagating systems. Thus, scientists need to describe these systems better. This paper offers one mechanism for the generation of these systems.

One necessary condition is more than normal rain just south of the Equator in the eastern Indian Ocean and less than normal rain centered over the Equator, south of India. This rain pattern is consistent with strong winds blowing to the east over Indonesia. However, this alone is not enough. These winds must be "pumped" towards the central Pacific. This is accomplished by switching the precipitation pattern described above on and off, essentially creating these bursts of wind every 30 to 60 days. These conditions were observed 8 and 6 months before the two strongest El Niños in the last 23 years, but were not observed with weaker El Niños. Thus, this mechanism is not foolproof for predicting El Niños, but it adds one piece to the bigger puzzle of El Niño.

Abstract

A pattern of variability in precipitation and 1000mb zonal winds for the tropical Indian Ocean during 1979 to 1999 (AtmIO mode) is described using EOFs. The AtmIO mode consists of a cross-equatorial gradient of precipitation anomalies and equatorial wind anomalies of alternating signs on the Equator. The positive phase is defined as enhanced precipitation to the south of the equator, suppressed precipitation to the north, and anomalous westerlies centered on the island of Sumatra. In September-October 1981, February-March 1990, and October-December 1996 the AtmIO mode was positive and there was a significant 30-60 day variability in the gradient of precipitation anomalies. These cases coincided with moderate to heavy activity in the Madden-Julian Oscillation (MJO). Links between the AtmIO, MJO, and El Niño are discussed.

1. Introduction

Recently, progress has been made towards characterizing internal modes of climate variability in the Indian Ocean. Webster et al. (1999) and Saji et al. (1999) observed an equatorial dipole of sea surface temperature (SST) with links to winds and precipitation, and proposed forcing mechanisms that would maintain this ocean-atmosphere interaction. Although this mode may lead to better climate predictions in the Indian Ocean region, it does not appear to be related to the El Niño / Southern Oscillation (ENSO) and would not improve the skill of such forecasts. This study complements Webster (1999) and Saji et al. (1999) by exploring atmospheric modes at higher frequencies.

Ever since Walker (1924) recognized the Southern Oscillation in trying to forecast Indian monsoon rainfall, there have been efforts to relate the climate of the Indian Ocean sector to

climate variations elsewhere (Rasmusson and Carpenter 1983, Webster and Yang 1992, Webster et al. 1998, Reason et al. 2000). Although much of the previous work has focused on the seasonal to interannual time scales, the eastern Indian Ocean is often a starting point for submonthly migrations of convection and the Madden-Julian Oscillation (MJO) (Madden and Julian 1994, Meehl et al. 1996).

From 21 years of Global Precipitation Climatology Project (GPCP) data (Huffman et al. 1997, Pingping Xie personal communication) and NCEP reanalysis winds (Kalnay et al. 1996), this study finds a mode of atmospheric variability in the tropical Indian Ocean sector that is distinct from the dipole mode proposed by Webster et al. (1999) and Saji et al. (1999).

2. Results

Figures 1a and 1b show the first and second EOFs of monthly precipitation (pEOF1, pEOF2) for the Indian Ocean domain (50-105E; 30N-30S). The pEOF1, with negative (positive) values in the eastern (western) Indian Ocean, is clearly a representation of the dipole mode, resembling Figure 4 in Saji et al. (1999). The pEOF2 explains almost 9% of the variance (Fig. 1b), and is a significant mode of variability according to the criteria of North et al. (1982). While pEOF1 is essentially a zonal gradient in precipitation anomalies, pEOF2 can be characterized as a Southeast-Northwest (SE-NW) gradient about the Equator.

The first four EOFs of zonal wind anomalies at 1000mb (u) were calculated. Table 1 shows the time series correlations between the wind EOFs and the first two precipitation EOFs (Figs. 1a,b). The temporal correlation between pEOF2 and the fourth EOF of u (uEOF4) is the only one that reaches the 1% significance level, using Quenouille's (1952) method to account for the resolution of effective number of degrees of freedom due to persistence. The time series

plots for these EOFs are shown in Fig. 1c. The correlation improves to +0.26 when precipitation leads the winds by a month. Overlain on pEOF2 is uEOF4 (Fig. 1b). The basin is dominated by negative (easterly) anomalies, with positive (westerly) anomalies south of 25S and at the Equator from 75E to 105E and near 50E. The pEOF2 and uEOF4 will be defined as the Atmospheric Indian Ocean (AtmIO) mode. Seasonal averages did not show a preferred season for the positive phase of the AtmIO mode (Fig. 1b). However the negative phase (opposite sign of Fig. 1b) is most likely to occur in boreal winter. This suggests some overlap between the negative phase of the AtmIO mode and the Indian Ocean dipole.

Fig. 2 shows the absolute magnitude of correlations between Nino 3.4 and the dipole and AtmIO modes, when the EOFs lead from 16 to 0 months. The Nino 3.4 autocorrelation is plotted as a measure of the skill of persistence. As noted by Saji et al. (1999) and Webster et al. (1999), the dipole pattern shows small correlation with ENSO. Although the AtmIO mode has equally small correlation, these values are better than persistence at a lead time of 9 to 14 months.

In order to explore the links between precipitation, equatorial wind, and ENSO in the eastern equatorial Pacific, the key feature of the AtmIO mode (the SE-NW gradient of precipitation anomalies) was reconstructed at a 5-day time step. The daily NCEP wind data was determined to be of lesser quality and thus not used. The SE-NW gradient of precipitation is assessed by computing the average anomaly within the Northwest box (NW, Fig. 1b) subtracted from the average anomaly within the Southeast box (SE, Fig. 1b). The time series of precipitation anomalies (Fig. 3a) shows a substantial amount of high frequency variability. A wavelet analysis (provided by C. Torrence and G. Compo and available at the URL http://paos.colorado.edu/research/wavelets) was performed on this time series (Fig. 3b). An inspection of the high frequencies (0.0312 to 0.125 years) reveals significant power (+90%) in

nearly all subseasonal bands at the end of 1981 and 1996. Fig. 4a shows the 30-60 day scale-average time series (thin line). Seven times during the record the mean 30-60 day power is well above the 95% confidence level. However, these peaks coincide with a strongly positive mean state of the AtmIO (thick line) only in 1981, 1990, and 1996. Fig. 4b shows a scatterplot of the time series in Fig. 4a. In general low-frequency variability is strong when high-frequency variability is weak and vice versa, as shown by the envelope of scatter. However, several points falling outside this envelope were identified as occurring in September-October 1981, February-March 1990, and October-December 1996 (Fig. 4b). For these cases the state of the gradient was positive and there was an enhancement of the 30-60 day variability. All were seasons of moderate to strong MJO activity and the 1981 and 1996 events led the onset of El Niño (Nino 3.4 > 0.5) by 8 and 6 months respectively.

3. Discussion

This study has identified consistent modes of variability between precipitation and 1000mb zonal wind in the tropical Indian Ocean region. The AtmIO mode is different from the dipole mode in many respects. The AtmIO mode is a purely atmospheric mode; the AtmIO mode has a pronounced meridional component; the AtmIO mode is not always tied to the annual cycle; and the AtmIO mode seems to lead the El Niño phenomenon by roughly a year. In the following discussion a mechanism linking the precipitation and zonal wind patterns is proposed. A physical connection to El Niño will also be suggested.

In the positive phase of the AtmIO mode the center of enhanced rainfall (Fig. 1b) is well south of the equator. This is consistent with the zonal wind pattern (Fig. 1b) which is positive to the north of the maximum precipitation anomaly and negative to the south (clockwise flow).

Secondly, the larger area of suppressed rainfall (Fig. 1b) sits on the equator and is accompanied by anomalous westerlies to the East and easterlies to the West, which is consistent with steady equatorial dynamics. It appears that the long-term (six months) average of this pattern of precipitation anomalies must be positive, and accompanied by a strong 30-60 day variability for there to be a subsequent connection to El Niño. We propose that the oscillation in precipitation pattern is accompanied by an oscillation in the sea level pressure pattern which serves as a "pump" for the surface westerlies over Sumatra. The time scale is consistent with the MJO, which has been observed to propagate from the Indian Ocean to the western Pacific (Weickmann and Khalsa 1990). It has been shown that winds in the far western Pacific have predictive skill for ENSO events, and in particular El Niños (Clarke and Van Gorder 2001). Therefore, the strength and subseasonal variability of the AtmIO mode could be used to predict (up to a year in advance) El Niño events that have their very beginnings in the Indian Ocean sector. However, further work is needed. Reliable observations of winds and atmospheric pressure, or appropriate regional modeling studies are required to advance our understanding of this mode of variability.

References

Clarke, A. J., and Van Gorder, 2001: ENSO prediction using an ENSO trigger and a proxy for western equatorial Pacific warm pool movement. Geophys. Res. Letters, 28, 579-582.

Huffman, G. J., R. F. Adler, P. Arkin, A. Chang, R. Ferraro, A. Gruber, J. Janowiak, A. McNab, B. Rudolf, U. Schneider, 1997: The Global Precipitation Climatology Project (GPCP) combined precipitation dataset. Bull. Amer. Meteor. Soc., 78, 5-20.

Kalnay, E., M. Kanamitsu, R. Kistler, W. Collins, D. Deaven, L. Gandin, M. Iredell, S. Saha, G. White, J. Woollen, Y. Zhu, M. Chelliah, W. Ebisuzaki, W. Higgins, J. Janowiak, K. C. Mo, C. Ropelewski, J. Wang, A. Leetmaa, R. Reynolds, R. Jenne, and D. Joseph, 1996: The NCEP/NCAR 40-year reanalysis project. Bull. Amer. Meteor. Soc., 77, 437-471.

Madden, R., and P. Julian, 1994: Observations of the 40-50-day tropical oscillation-A review. Mon. Wea. Rev., 122, 814-837.

Meehl, G. A., G. N. Kiladis, K. M. Weickmann, M. Wheeler, D. S. Gutzler, and G. P. Compo, 1996: Modulation of equatorial and subseasonal convective episodes by tropical-extratropical interaction in the Indian and Pacific Ocean regions. J. Geophys. Res., 101, 15033-15049.

North, G. R., T. L. Bell, R. F. Cahalan, and F. J. Moeng, 1982: Sampling errors in the estimation of empirical orthogonal functions. Mon. Wea. Rev., 110, 699-706.

Quenouille, M. H., Associated Measurements, 242 pp., Butterworths, London, 1952.

Rasmusson, E. M., and T. H. Carpenter, 1983: The relationship between eastern equatorial Pacific sea surface temperature and rainfall over India and Sri Lanka. Mon. Wea. Rev., 111, 517-528.

Reason, C. J. C., R. J. Allan, J. A. Lindesay, and T. J. Ansell, 2000: ENSO and climatic signals across the Indian Ocean basin in the global context: Part I, interannual composite patterns. Int. J. Climatol., 20, 1285-1327.

Saji, N. H., B. N. Goswami, P. N. Vinayachandran, and T. Yamagata, 1999: A dipole mode in the tropical Indian Ocean. Nature, 401, 360-363.

Walker, G. T., 1924: Correlation in seasonal variations of weather IX. Mem. Indian Meteor. Dept., 20, part 6, 117-124.

Webster, P. J., V. O. Magaña, T. N. Palmer, J. Shukla, R. A. Tomas, M. Yanai, and T. Yasunari, 1998: Monsoons: Processes, predictability, and the prospects for prediction. J. Geophys. Res., 103, 14451-14510.

Webster, P. J., A. M. Moore, J. P. Joschnigg, and R. R. Leben, 1999: Coupled ocean-atmosphere dynamics in the Indian Ocean during 1997-98. Nature, 401, 356-360.

Webster, P. J., and S. Yang, 1992: Monsoon and ENSO: Selectively interactive systems. Quart. J. Roy. Meteor. Soc., 118, 877-926.

Weickmann, K. M., and S. J. S. Khalsa, 1990: The shift of convection from the Indian Ocean to the western Pacific Ocean during a 30-60 day oscillation. Mon. Wea. Rev., 118, 964-978.

Figure Captions

Figure 1. The first and second EOFs of precipitation (pEOF1, pEOF2) and fourth EOF of 1000mb zonal wind (uEOF4) anomalies in the Indian Ocean sector. A) pEOF1 (explains 18.1% of the variance). B) Color shading denotes pEOF2 (explains 8.7% of the variance) and contour lines denote uEOF4 (explains 7.2% of the variance). Boxes indicate areas used to define the SE-NW gradient in precipitation anomalies. C) Time series of pEOF2 (dashed line) and uEOF4 (solid line).

Figure 2. Absolute magnitude of time-lag correlations. Solid line is the autocorrelation of Nino 3.4 from 0 to 16 months. Long-dashed line is the correlation between Nino 3.4 and pEOF1 when pEOF1 leads by 0 to 16 months. Short-dashed line is the correlation between Nino 3.4 and

pEOF2 when pEOF2 leads by 0 to 16 months. Dot-dashed line is the correlation between Nino 3.4 and uEOF4 when uEOF4 leads by 0-16 months.

Figure 3. Analysis of 5-day time series of the SE-NW gradient of precipitation anomalies (see boxes in Fig. 1b). A) Raw time series of the SE-NW gradient. B) Morlet wavelet power spectrum of the raw time series in (A). The contour levels are chosen so that 75%, 50%, 25%, and 5% of the wavelet power is above each level, respectively. Cross-hatched region is the cone of influence, where zero padding has reduced the variance. Black contour is the 10% significance level, using the global wavelet spectrum as the background.

Figure 4. Relationship between the power of 30-60 day oscillations and long-term running average of the SE-NW gradient of precipitation anomalies. A) Thin line denotes time series of the 30-60 day scale-average of the wavelet power spectrum in Fig. 4b. Thick line denotes time series of the six month running mean of the SE-NW gradient of precipitation anomalies (Fig. 4a). B) Scatterplot of the two time series in (A), showing precipitation anomalies as a function of 30-60 day power. Certain data points are identified with open circles, squares, and diamonds

Table 1. Correlations between precipitation and u EOFs

	uEOF1	uEOF2	uEOF3	uEOF4
pEOF1	-0.09	+0.19	-0.03	-0.05
pEOF2	+0.01	-0.10	+0.05	+0.23

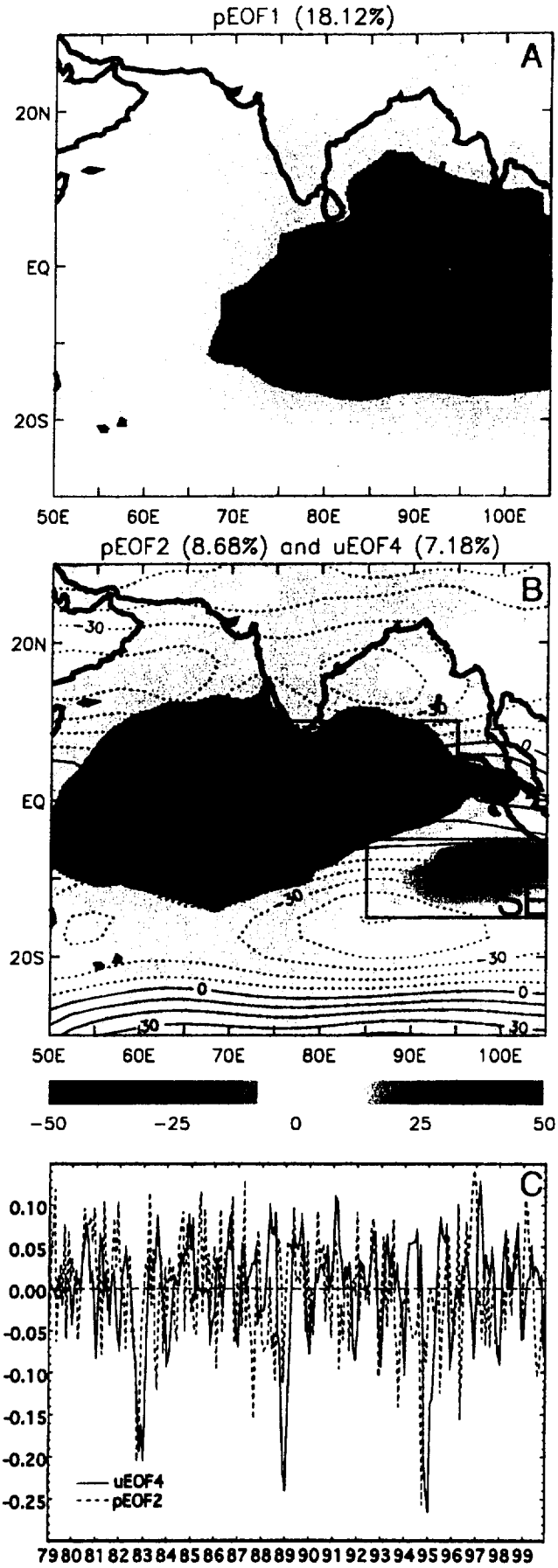
pEOF1 (18.12%)
A
20N
EQ
20S
50E
60E
70E
80E
90E
100E
pEOF2 (8.68%) and uEOF4 (7.18%)
B
-30
0
SE
-50
-25
0
25
50
C
0.10
0.05
0.00
-0.05
-0.10
-0.15
-0.20
-0.25
uEOF4
pEOF2
79 80 81 82 83 84 85 86 87 88 89 90 91 92 93 94 95 96 97 98 99

FIG 2

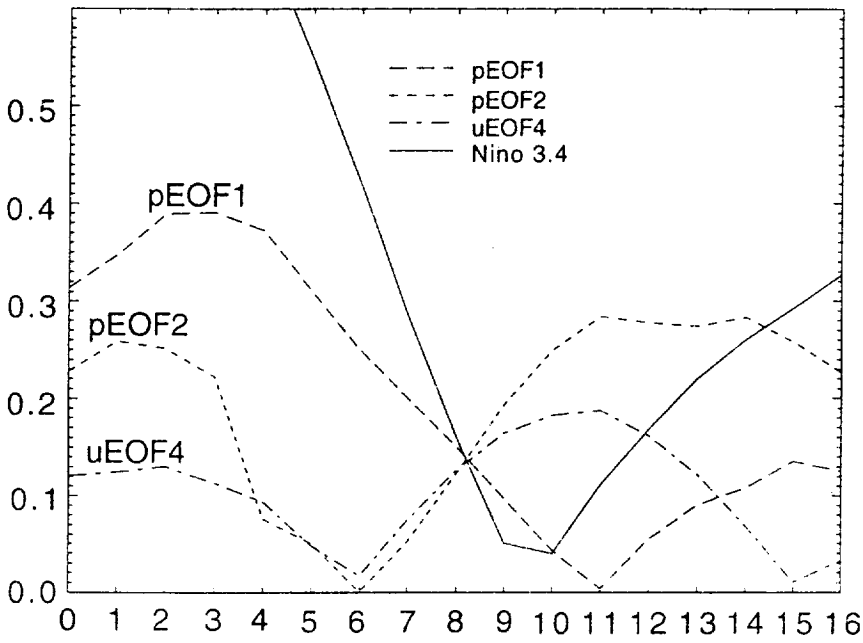
pEOF1
pEOF2
uEOF4
Nino 3.4
pEOF1
pEOF2
uEOF4
0.5
0.4
0.3
0.2
0.1
0.0
0 1 2 3 4 5 6 7 8 9 10 11 12 13 14 15 16

FIG 3

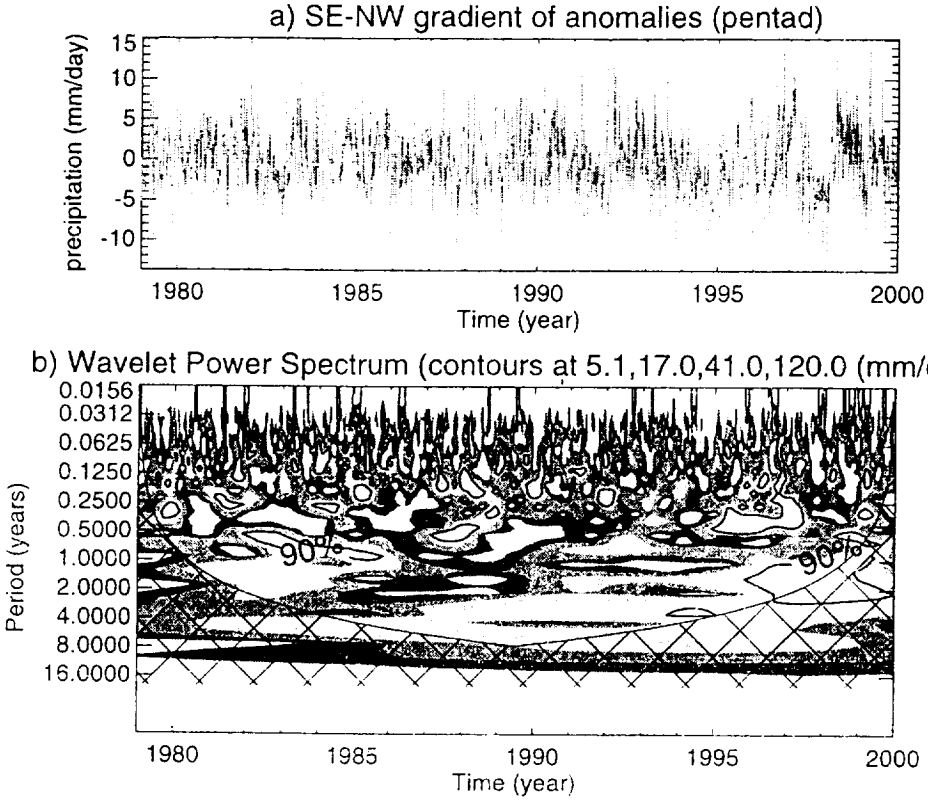
a) SE-NW gradient of anomalies (pentad)
precipitation (mm/day)
15
10
5
0
-5
-10
1980
1985
1990
1995
2000
Time (year)
b) Wavelet Power Spectrum (contours at 5.1,17.0,41.0,120.0 (mm/day)^2)
Period (years)
0.0156
0.0312
0.0625
0.1250
0.2500
0.5000
1.0000
2.0000
4.0000
8.0000
16.0000
90%
90%
1980
1985
1990
1995
2000
Time (year)

FIG 4

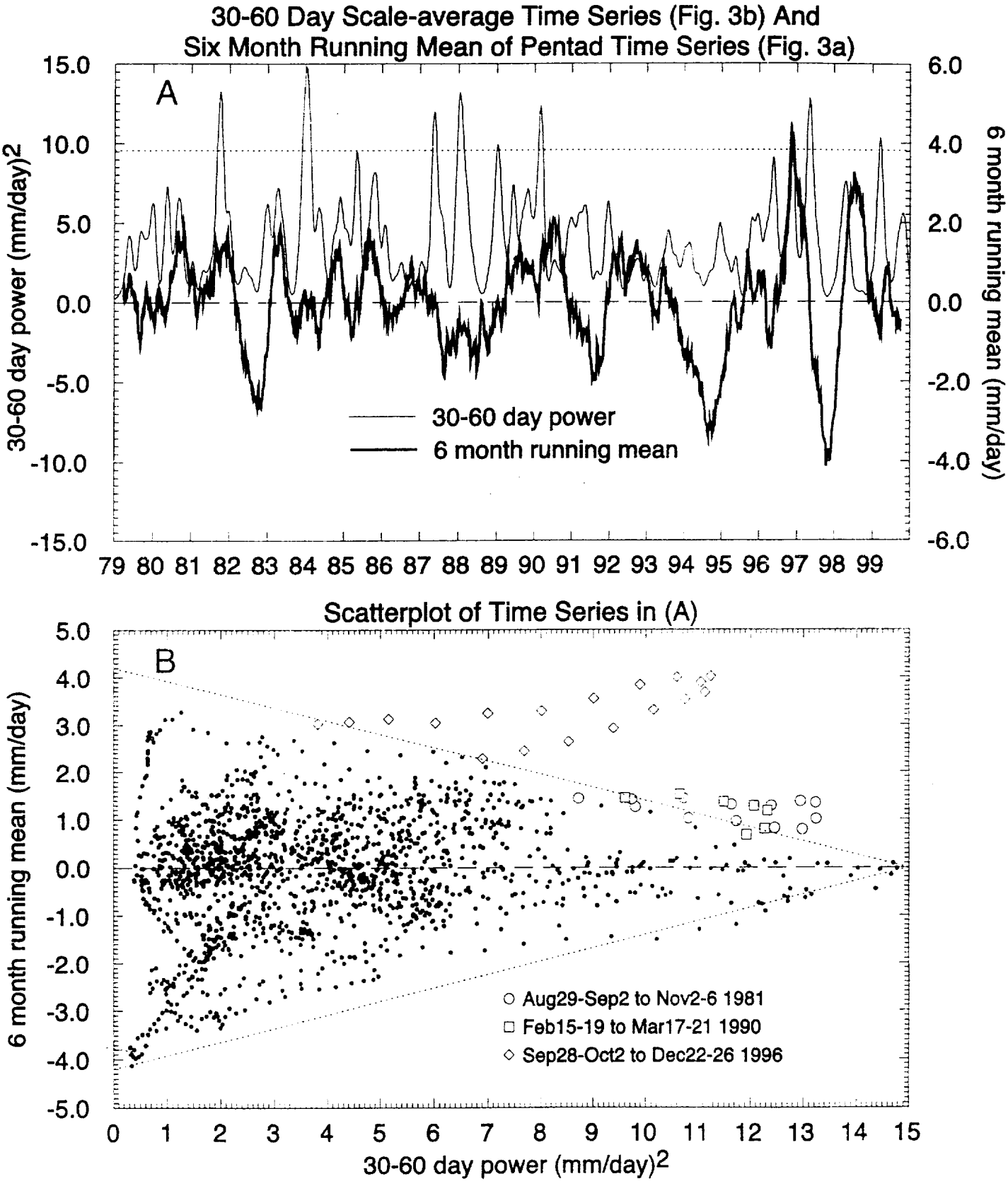
30-60 Day Scale-average Time Series (Fig. 3b) And
Six Month Running Mean of Pentad Time Series (Fig. 3a)
A
30-60 day power (mm/day)2
6 month running mean (mm/day)
15.0
10.0
5.0
0.0
-5.0
-10.0
-15.0
6.0
4.0
2.0
0.0
-2.0
-4.0
-6.0
30-60 day power
6 month running mean
79 80 81 82 83 84 85 86 87 88 89 90 91 92 93 94 95 96 97 98 99
Scatterplot of Time Series in (A)
B
6 month running mean (mm/day)
5.0
4.0
3.0
2.0
1.0
0.0
-1.0
-2.0
-3.0
-4.0
-5.0
Aug29-Sep2 to Nov2-6 1981
Feb15-19 to Mar17-21 1990
Sep28-Oct2 to Dec22-26 1996
0 1 2 3 4 5 6 7 8 9 10 11 12 13 14 15
30-60 day power (mm/day)2

PRECIPITATION ANOMALIES IN THE TROPICAL INDIAN OCEAN AND POSSIBLE LINKS TO THE INITIATION OF EL NIÑO

Scott Curtis[1]

Joint Center for Earth Systems Technology, University of Maryland Baltimore County, Baltimore, Maryland

Robert F. Adler

NASA Goddard Space Flight Center, Greenbelt, Maryland

George J. Huffman[1]

Science Systems and Applications Inc., Lanham, Maryland

[1]Also at NASA Goddard Space Flight Center, Greenbelt, MD

Submitted to Geophysical Research Letters, May 3 2001